

Determination Of Covid-19 Pulmonary Infection Rate From X-Ray Images Using U-Net Model

Mohammed S. H. Al-Tamimi^{1*}, Hadeel Jabar², Husam Ali Abdulmohsin³, Farah khiled AL-Jibory⁴

Computer Science Department, College of Science, University of Baghdad, Baghdad, Iraq¹²³

Ministry of Education, Karkh First Directorate of Education, Baghdad, Iraq⁴

mohammed.s@sc.uobaghdad.edu.iq¹, hadeel.jriash@sc.uobaghdad.edu.iq²,

Husam.a@sc.uobaghdad.edu.iq³, csd1b0037@gmail.com⁴

Received: 04 December 2024, Revised: 02 April 2025, Accepted: 13 April 2025

*Corresponding Author

ABSTRACT

Global health has suffered by millions of COVID-19 infections and fatalities. Pneumonia and ARDS are major consequences of this viral infection. Patient treatment and resource allocation depend on accurate lung infection rates. Reverse transcription polymerase chain reaction (RT-PCR) is highly specific but lacks sensitivity, especially in early infection. Thus, imaging, particularly chest X-rays, is crucial for detecting and monitoring COVID-19-related pulmonary problems. Among various image processing techniques, deep learning methods, especially U-net models, have shown promising results in segmenting and analyzing X-ray images to determine the extent of lung infection. This article explores the importance of imaging techniques in diagnosing COVID-19 lung infection, provides an overview of the U-Net model in medical imaging, and describes in detail the method of using this complex model to determine infection rates from radiographs. This study discusses the diagnosis of coronavirus infection, i.e. whether a person is infected or not, and determines the infection rate (severity) that mean the percentage of virus in the lungs was calculated based on a global radiograph (X-ray) dataset to study the infection, infection rate, and diagnosis by specialists using a pre-trained model (U-Net model). The results obtained were 97% accurate in diagnosing whether a patient was infected with the virus or not.

Keywords: COVID-19, Diagnosis, Severity, Data, Squeeze Net Model.





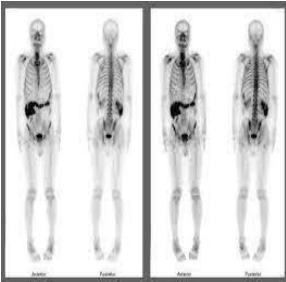
1. Introduction

In 2019, a pneumonia outbreak occurred. Epidemiological studies have shown an association between the Huanan Seafood Wholesale Market and an epidemic of pneumonia cases. A new respiratory virus was discovered by inhalation of material from human lung cell lines, particularly the Verda Reno cell lines (Vero E6 and Huh7) (X. Jiang et al., 2021) Analysis of the viral genome showed that it was a newly discovered coronavirus, closely related to SARS-CoV (Kovács et al., 2021). As a result of subsequent discoveries, the virus was named severe acute respiratory syndrome coronavirus. Due to the large number of deaths caused by Covid-19 and the widespread spread of the virus, it has become a high risk. On March 12, 2020, the World Health Organization officially declared a global pandemic (Xu et al., 2022). The outbreak has had a serious impact on the world, especially the loss of life, economic impact, and high poverty rates. Pneumonia is the main clinical manifestations of COVID-19, which is associated with SARS-CoV-2 and helps in case detection (Mehraeen et al., 2020). Recently, there has been an increase in gastrointestinal symptoms and asymptomatic infections, especially in young children. The average incubation period appears to be 5 to 7 days, while the median incubation period is 3 days (range 0 to 24 days (Al Jibory et al., 2022) This information is based on observations to date. It is not yet clear what percentage of people infected with Covid-19 will remain asymptomatic throughout their illness (Mehboob et al., 2022). Clinical manifestations of the disease include upper respiratory tract infection symptoms such as fever, cough, nasal congestion, and fatigue, which usually occur within a week of the patient's first symptoms of the disease (Sufian et al., 2023) Severe illness may present with difficulty breathing and severe chest symptoms (suggesting pneumonia). The second or third week after infection is usually when pneumonia symptoms become severe and severe (khiled AL-Jibory et al., 2022). Early symptoms of viral pneumonia include decreased oxygen saturation, changes in blood gas levels, and changes on chest X-rays and other imaging tests. Changes include changes in ground-glass

opacity, scattered consolidation, fluid accumulation within the alveoli, and demarcation of the interlobular spaces(Al Jibory et al., 2022). All of these indicate that the patient is getting worse. Changes in blood pressure are another sign. All these symptoms can be avoided by early detection, X-ray is one of the most cost-effective methods of medical imaging procedures, and is adopted due to its reasonable price and diagnostic accuracy, since through X-ray it is possible to detect the presence of pneumonia, even at the beginning of symptoms or in the early stages (Slika et al., 2023).Therefore, due to the rapid development of technology worldwide, developed countries have turned to the use of artificial intelligence to determine the infection rate through algorithms designed to determine the presence of infection, and it is possible to determine the infection rate. Because this epidemic has completely changed the characteristics and development trends of the earth and the security of world information maintenance. People are protected from infection(Mijwil et al., 2022). In recent years, deep learning has revolutionized medical imaging, particularly in identifying COVID-19 from chest X-rays and CT scans. Numerous studies have demonstrated the effectiveness of convolutional neural networks (CNNs) and other deep learning models in identifying COVID-19 infections. Several researchers have proposed a deep learning methodology that uses convolutional neural networks to classify chest X-rays into COVID-19 and non-COVID-19 categories, achieving high accuracy(Talukder et al., 2024). A CNN model has been specifically used to identify COVID-19 pneumonia from X-rays, demonstrating the effectiveness of deep learning models for rapid and reliable diagnosis, especially in resource-limited settings(Kashyap et al., 2024). Despite the encouraging results, these studies often face several problems, including limited dataset size, model overfitting, and difficulties in generalizing across diverse populations. Although many models focus primarily on binary classification (COVID-19 vs. non-COVID-19), few address infection severity, which is fundamental for patient management and clinical decision-making. Recent developments have sought to mitigate these limitations by applying transfer learning techniques and leveraging larger datasets, with a focus on models such as U-Net for segmenting and quantifying infection severity(Kashyap et al., 2024). These initiatives underscore the growing importance of AI and deep learning in the early detection and management of COVID-19, providing potential solutions to the urgent demand for rapid and accurate diagnostic tools during the pandemic. In this paper, This study presents an innovative technique utilizing a pre-trained U-Net model to analyze chest X-rays for the detection and assessment of pneumonia associated with COVID-19, diverging from prior research that primarily concentrated on binary classification (pneumonia vs. non-pneumonia) and utilized limited datasets, such as chest X-rays. Prior research has demonstrated encouraging outcomes utilizing deep learning for COVID-19 identification (Wang et al., 2020; Zhang et al., 2020); nevertheless, numerous models experience overfitting challenges attributable to limited and imbalanced datasets. The severity of infection is crucial for patient treatment and prognosis, however it is frequently neglected. Our research fills this gap by utilizing an extensive worldwide dataset and comprehensive infection severity evaluations, proposing a dual strategy encompassing infection detection and severity assessment.

2. Medical Image Types and deep learning methods

Medical imaging refers to the process and methodology of capturing images inside the body for clinical examination and medical treatment It also allows for visual depiction of the operation of certain organs or tissues (physiology). The medical imaging aims to unveil underlying structures obscured by the skin and bones, as well as to diagnose and treat illnesses. Medical imaging also creates a repository of typical anatomical and physiological data, enabling the detection of anomalies)(Alia et al., 2020). While it is possible to do medical imaging of extracted organs and tissues for diagnostic purposes. Table 1 summarized Difference Types of Medical Image that is commonly used in diagnosing lung diseases.

Table 1 - Summarized Difference Types of Medical Image		
Type	Description	Image
X-RAY	One type of ionizing radiation that can enter the human body is X-rays. The most common and traditional type of medical imaging is X-rays, utilized to generate images of bones, teeth, and other solid tissues. They are relatively affordable and straightforward to execute. Nevertheless, their capability is limited to generating visual representations of compact tissues, such as bones and teeth(Chen et al., 2020)	
CT SCAN	The computed axial tomography scan or CAT scan (CT) scans are costlier than X-rays, although they have the capability to generate far more intricate images of the internal structures of the body. They are frequently employed for the purpose of diagnosing cancer, heart disease, and various other medical disorders (Xu et al., 2022). CT scans employ X-rays to create complete images of the body's interior structures. They are frequently employed for the purpose of diagnosing cancer, heart disease, and various other medical disorders(Qadir et al., 2024)	
MRI	Magnetic Resonance Imaging (MRI) employs magnetic fields and radio waves to generate visual representations of the internal structures of the human body. They are frequently employed for the purpose of diagnosing soft tissue ailments, such as torn ligaments or herniated discs. Magnetic Resonance Imaging (MRI) is the costliest form of medical imaging. Nevertheless, they possess the ability to generate highly intricate visual representations of the inside structures of the body, encompassing delicate tissues. Magnetic resonance imaging (MRI) is frequently employed for the purpose of diagnosing brain cancers, spinal cord injuries, and various other medical disorders(Al-Tamimi & Sulong, 2014)	
Ultra sound	Ultrasound is a secure and non-invasive form of medical imaging commonly employed for pregnancy diagnosis and fetal development monitoring. Additionally, it can be utilized to scrutinize inside organs, including the liver, kidneys, and uterus. Furthermore, Acoustic waves are used in ultrasound to create visual depictions of the body's internal systems. It is frequently employed for the purpose of diagnosing pregnancy, monitoring fetal development, and examining internal organs (Gayathri et al., 2023)	
Nuclear	Nuclear medicine use radioactive tracers to generate internal body imaging. It is frequently employed for the purpose of diagnosing cancer, heart disease, and various other medical disorders. Furthermore Nuclear medicine use radioactive tracers to generate internal body imaging. The tracers are administered intravenously and subsequently absorbed by targeted tissues. The tracers release radiation that is detectable by a specialized camera. Nuclear medicine is frequently employed for the purpose of diagnosing cancer, cardiovascular disease, and various other medical disorders(Seibert & Boone, 2005)	

There are several different kinds of deep learning models used to identify pneumonia; this pint gives a quick summary of them, along with their advantages and disadvantages.

- Convolutional neural networks (CNNs) are extensively employed for pneumonia detection in chest X-rays. They can effectively extract features and classify photos with considerable precision. Nonetheless, CNNs are susceptible to overfitting when trained on limited datasets and frequently struggle to generalize across diverse populations. They also exhibit a deficiency in interpretability, complicating physicians' comprehension of modeling judgments.
- U-Net is a deep learning architecture specifically designed for image segmentation, demonstrating high efficacy in identifying and delineating pneumonia zones in X-ray images. The U-Net model, while exhibiting precise localization capabilities, is fundamentally intended for segmentation tasks.

- ResNet (residual network) incorporates a deeper architecture with skip connections to enhance feature extraction and model resilience. It is adept at handling extensive datasets and intricate features; yet, it demands substantial processing resources, rendering it inappropriate for real-time applications. Moreover, it may experience overfitting issues when trained on tiny or imbalanced datasets.
- VGGNet is recognized for its profound architecture utilizing a compact 3x3 filter for pneumonia detection in chest X-rays. It has robust efficacy in classification tasks; nevertheless, it is computationally intensive and not tailored for medical imaging, rendering it less appropriate for real-time applications.
- DenseNet interlinks every layer, enhancing feature reutilization and attaining superior performance with a reduced number of parameters. Nonetheless, DenseNet models are resource-intensive and may exhibit suboptimal performance on limited datasets, constraining their applicability in clinical environments.
- XceptionNet employs depthwise separable convolutions to diminish computing complexity while maintaining excellent accuracy in pneumonia identification. XceptionNet necessitates extensive, high-quality datasets for optimal training and exhibits subpar performance on limited, noisy data, posing challenges in medical imaging.
- SqueezeNet is an efficient model designed for resource-constrained environments. It is economical and performs effectively on smaller datasets; nevertheless, its accuracy is typically inferior to that of more intricate models like ResNet or DenseNet. It also exhibits subpar performance on tasks necessitating fine-grained classification.
- YOLO (You Only Look Once) is a real-time object detection approach utilized for pneumonia identification in chest X-rays. It facilitates rapid detection with great precision; but, it is inadequate for applications necessitating pixel-level classification or segmentation, hence constraining its utility in intricate medical diagnostics.

3. Literature Review

Were studies that had an impact by previous researchers about diagnosing the Covid virus in terms of infection, and they were studies that had an impact. Below are the most important studies that were close to the proposed work:

- Gayathri J.L et al. (2022) (Gayathri et al., 2023) proposes a computer-aided detection technique that uses images from chest X-rays to fight the pandemic. To create the model, a number of pre-trained networks and their combinations were employed. The technique makes use of features taken from pre-trained networks, a feed forward neural network (FFNN) for COVID-19 detection, and a sparse autoencoder for dimensionality reduction. The model has been trained using two publicly accessible datasets of chest X-ray pictures, which include 504 COVID-19 images and 542 non-COVID-19 images.
- Mohamed Loey et al. (2022) (Khalifa et al., 2022) there are two major parts to the proposed paradigm. The first one learns and extracts deep features using CNN. A Bayesian-based optimizer comprises the second part, which is utilized to adjust the CNN hyperparameters based on an objective function. 10,848 photos make up the big, well-balanced dataset that was used.
- Seyed Mohammad Jafar Jalali et al. (2022) (Dipu Kabir et al., 2023) provide a workable solution for using convolutional neural networks (CNNs) to analyze chest X-ray pictures in order to diagnose COVID-19 disease to enhance the competitive swarm optimizer's basic version in order to increase accuracy and create a fresh evolutionary method.
- Oussama Aiadi et al. (2022) (Aiadi et al., 2023) suggests using telemedicine to diagnose COVID-19 and lung disorders using a computationally quick network. Because it simultaneously encodes local binary patterns and the filter outputs of the discrete cosine transform (DCT), the proposed network is known as Deep Learning Network (DLNet). The convolution layer, which makes up the first layer in DLNet, uses DCT filters to convolve the input image. Afterward, to prevent overfitting. The process of binary hashing involves combining the output of several filters to create a distinct feature map.
- Isaac Ariza et al , (2022) (Ariza et al., 2023) recommended technique for identifying mental activity is provided: Using bidirectional LSTM neural networks, instantaneous frequency,

spectral entropy, and Mel-frequency cepstral coefficients (MFCC) are utilized to identify EEG signals, electroencephalography (EEG) paired with deep learning is a powerful technology that lets us investigate brain activity at a high temporal resolution.

- Somenath Chakraborty et al. (2022) (Chakraborty, 2022) Chest X-ray (CXR) pictures were used to identify COVID-19 using a Deep Learning Method (DLM) for COVID-19 detection in contrast to other costly and time-consuming pathological procedures used for quick examination of CXR pictures, allowing radiologists to quickly screen possible candidates for COVID-19 detection. Table 2 summarized the above related work in topic Diagnosing covid-19.

Table 2 - Summary of Related Work

Refers	Method	Dataset	Illustration	Result
Gayathri J.L et al. (2022) (Gayathri et al., 2023)	CNN integration with feed forward neural network and sparse autoencoder	X-ray image COVID-19	To create the model, a number of pre-trained networks and their combinations were employed	Accuracy= 0.9578 F1-Score=0.9563 Precision=0.9563 AUC=0.9821
Mohamed Loey et al. (2022) (Khalifa et al., 2022)	There are two major parts to the proposed paradigm. In the first, deep features are extracted and learned via CNN. A Bayesian-based optimizer is the second part, and it is used to adjust the CNN hyperparameters based on an objective function. 10,848 photos make up the large-scale, well-balanced dataset that was employed	X-ray image COVID-19	Compared three different ablation scenarios to Bayesian optimization	Accuracy = 0.96 F1-Score=Not Used Precision=Not Used AUC=Not Used
Seyed Mohammad Jafar Jalali et al. (2022) (Dipu Kabir et al., 2023)	utilizing a convolutional neural network (CNN) to analyze the X-ray pictures of the chest	X-ray image COVID-19	Create a new evolutionary algorithm by enhancing the competitive swarm optimizer's foundational version	Accuracy = 0.985 Precision= 0.988024 AUC= 0.985547 F1 = 0.985075
Oussama Aiadi et al. (2022) (Aiadi et al., 2023)	rapid network for pulmonary disease and COVID-19 detection that can be utilized in telemedicine	X-ray image COVID-19	It simultaneously encodes the filter outputs of the discrete cosine transform (DCT) and local binary patterns.	Precision = 98.06 Recall = 99.24% F-1= Not Used Accuracy = 98.86
Isaac Ariza, (2022) (Ariza et al., 2023)	local density depth feature nverse Path Length	X-ray image COVID-19	Electroencephalography (EEG) paired with deep learning is a technology that allows us to evaluate brain activity with high temporal resolution.	Precision = 0.94 Recall = Not used F-1 = 0. 78 Accuracy = Not used
Somenath Chakraborty et al. (2022) (Ariza et al., 2023)	Applied Deep Learning Techniques (DLM)	COVID-19	quick examination of CXR images, allowing radiologists to quickly screen possible	Precision = 0.93 Recall = 0. 93. F-1= 0.87 Accuracy = 0. 96.

candidates and
identify COVID-
19

Despite advances in deep learning pneumonia detection models, numerous major gaps remain in current research. First, most studies detect pneumonia or COVID-19 but not infection severity, which is crucial for patient treatment and clinical decision-making. Second, many models have short and imbalanced datasets, which cause overfitting and poor generalization, especially when tested across populations or medical imaging situations. CNNs, U-Net, and ResNet can categorize pneumonia, but they cannot estimate infection extent, which is crucial for disease development. While successful, previous models demand substantial processing power, rendering them unsuitable for real-time clinical applications, especially in resource-limited situations. Segmentation methods like U-Net have been used to detect pneumonia in X-rays, but most studies have not integrated them with classification or severity analysis, limiting their clinical relevance. This paper proposes a complete method that detects pneumonia and scores infection severity to fill these gaps. This gives models clinical importance they lack. The work ensures model generalizability and robustness by using a larger and more diversified dataset. Pre-trained U-Net design accurately segments contaminated areas, boosting pneumonia localization and diagnostic accuracy. The model has been refined to lower computing costs, allowing quick diagnosis in resource-limited situations and boosting its application in various healthcare settings. These improvements make the suggested approach more complete, practical, and adaptable to various clinical use cases.

4. The Proposed System

Proposed an artificial intelligence system that utilizes spatially deep learning. This system employs a pre-training model and utilizes a standardized and global dataset with spatial attributes. The dataset includes images for detecting COVID-19 through X-ray scans and comma-separated values (CSV) files for assessing severity. The suggested method consists of four stages: data pruning, image pre-processing, classification for detecting COVID-19, and regression for determining severity. The final stage involves prediction. This stage involves the creation of content sub-stages that are supported by graphical interfaces designed to enhance user productivity. Figure 1. Shows the Structural of proposed system.And This study's innovation is the development of a mechanism for evaluating pneumonia severity, which has been largely neglected in prior research. Utilizing a larger and more diverse dataset improves the model's generalizability, while integrating segmentation with classification and severity analysis yields a more thorough diagnostic instrument. These enhancements render the proposed model more therapeutically practical, efficient, and resilient, particularly in real-time, resource-limited environments.

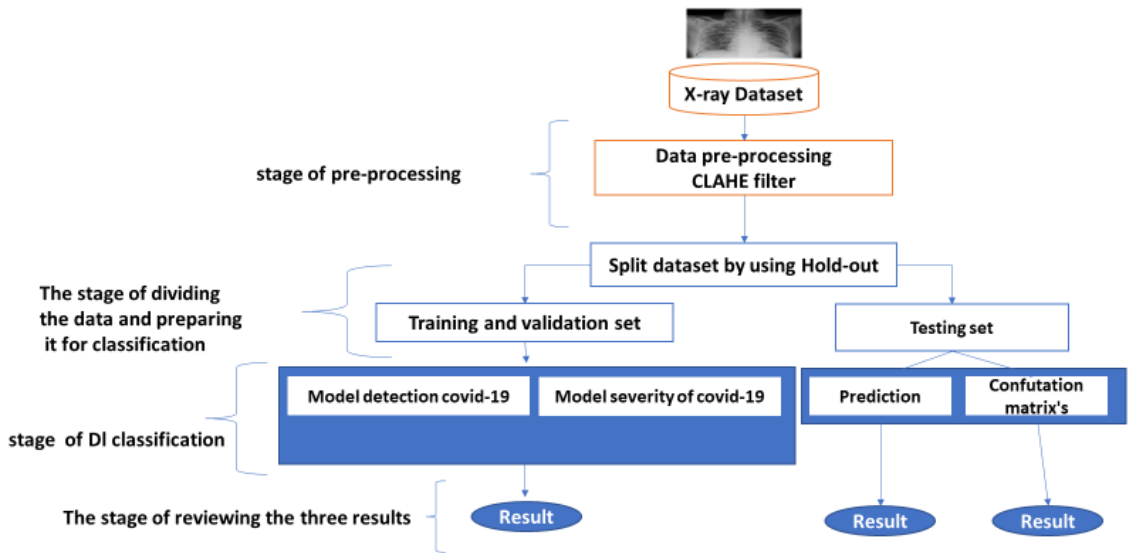


Fig. 1. Structural Of Proposed System.

Based on above figure can summarized the scope of proposed approached is: Generalization across diverse populations:

- It uses a larger and more diverse dataset, including demographic data and different severity levels, to improve model generalization. These datasets have been challenging for researchers due to their in-depth detail.
- Data Imbalance and Limited Datasets:
- It uses a comprehensive and balanced dataset, which reduces overfitting and enhances model robustness. This means it contains a consistent number of data points across infection and severity for fair training.
- Interpretability and Confidence:
- It incorporates a U-Net segmentation architecture, providing clear and interpretable visual maps of infection areas. The use of this type of model is novel in the diagnosis of multiple lung infections.
- Severity Assessment and Disease Progression:
- It provides a severity scoring mechanism to assess the extent of infection and support clinical decision-making. This is the most important aspect, as severity was assessed using x-ray images, an alternative to CT scans, which are expensive or more research-intensive in lung cancer. Previous studies have not focused on measuring the severity of the injury, but rather on whether the patient is infected or not.
- Robustness to Noisy or Low-Quality Data:
- CLAHE preprocessing is applied to improve image quality, which improves robustness to noisy data. Combining it with other techniques results in a highly effective processing mechanism.
- Model Bias and Fairness:
- It is trained on a diverse dataset to reduce bias and ensure fair and equitable predictions across different population groups.
- Training:
- The most important point is that the proposed approach involves several efficient processing operations. Two models were used, one to determine whether a patient is infected or not, and the other to assess the severity of the injury. The result is a single result similar to the medical report generated by a CT scan, which is the injury and its impact on the lung.

5. Dataset and Pre-Processing in Proposed System

In the proposed system, a data set (Covid-19 Xray Severity Scoring) was adopted, which is distinguished from others in that it contains a real infection rate diagnosed by doctors and contains infected and uninfected people of different ages of men, women and children. Table 3 showing the complete details of the approved data set that used in proposed approaches.

Table 3 - Dataset Details						
File name	Study Date	Modality	Manufacturer	Photometric Interpretation	Score Global sort	Test set sort
File path	Filename	DICOM Photometric interpretation (already preprocessed, so you do not have to worry about this)	Original Image Width	Original Height	ImageOverall Severity Score	The consensus test set is the proper testing set - evaluated by five radiologists rather than one elsewhere.
4695 unique values	4695 unique values	-CR (Computed Radiography)	SIEMENS Agfa Carestream Health	Monochrome1	4695 unique values	(0 or 1)
		-DX (Digital experience)	Carestream Health Agfa-Gevaert	Monochrome2	(1-18)	

in the proposed system, the CLAHE filter was adopted. The CLAHE filter, or Contrast Limited Adaptive Histogram Equalization, is an effective image processing technique used to improve the local contrast of the image, especially in areas with low contrast (Al-Tamimi & AL-Khafaji, 2022). In short, it is a filter or algorithm that works to balance the contrast of images, that is, it works. It lightens the dark area and darkens the light area, and it is based on the concept of Clip Limit Parameter (CLP). Is denoted by equation 1 (Setiawan et al., 2013)

$$CLP = \left\lfloor \frac{w}{256} \right\rfloor + \left\lfloor \beta \cdot \left(w - \frac{w}{256} \right) \right\rfloor \dots \dots \dots (1)$$

Where:

w Denotes the size of the tile or window area that has to be considered, β is the pre-defined CL

This method is an improvement over the traditional adaptive histogram equalization (AHE) technique, because it effectively mitigates the problem of excessive noise amplification and artifacts that can arise with AHE (Al-Khafaji & Al-Tamimi, 2022). The following point description the steps of CLAHE filter work that lead to use in proposed system.

- 1- Split the image up into tiny, non-overlapping tiles: The image is split up into a grid individual tiles, each representing a local area.
- 2- Determine the histogram for every tile: Every tile's histogram is computed representing the distribution of intensity values within that specific area.
- 3- Apply histogram equalization to each tile: Each tile's histogram is equalized using a traditional histogram equalization method. This stretches the intensity values to fill the full range, enhancing local contrast.
- 4- Limit the contrast amplification: In CLAHE, a clipping process is applied to the equalized histogram to limit the maximum intensity value. This prevents the over-amplification of noise and artifacts.
- 5- Combine the tiles back into the final image: The processed tiles are then combined back together to form the final enhanced image.

Figure 2 shows the effected of filter CLAHE in proposed system.

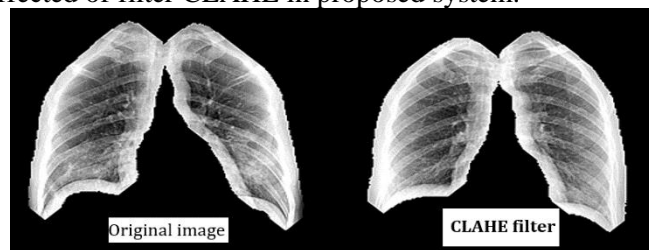


Fig. 2. Original Image in Dataset and CLAHE Filter

The idea of using this type of filter is to create a balance for grayscale images, so it works to lighten the dark areas and darken the light areas in a balanced way. After performing the initial data preparation operations, the division process of the data into a test set and a training set will take place. This will be done based on the k-fold technique, with five experiments. This method was adopted because the division is more accurate and proportional to the size of the database.

6. Training stage in proposed system

The study “U-Net: Convolutional Networks for Biomedical Image Segmentation” established the widely used deep learning architecture U-Net. This design aims to overcome medical data shortages. The network uses small amounts of data efficiently while retaining speed and accuracy. A contracting path and an expanding path make U-Net's architecture distinctive. The expanding path contains decoder layers that decode encoded data and generate segmentation maps using skip connections from the contracting path, while the contracting path encodes contextual information and reduces input spatial resolution. U-Net's contracting path finds relevant image features. The encoder layers convolutionally lower feature map spatial resolution and increase depth, collecting progressively abstract input representations. Other convolutional neural networks have feed-forward layers like this contracting path. However, the expanding path decodes and localises information while maintaining input spatial resolution. Feature map upsampling and convolution are performed by increasing path decoder layers.

Figure 3 shows how skip connections from the contracting path maintain spatial information lost in the path, helping the decoder layers localise features more precisely.

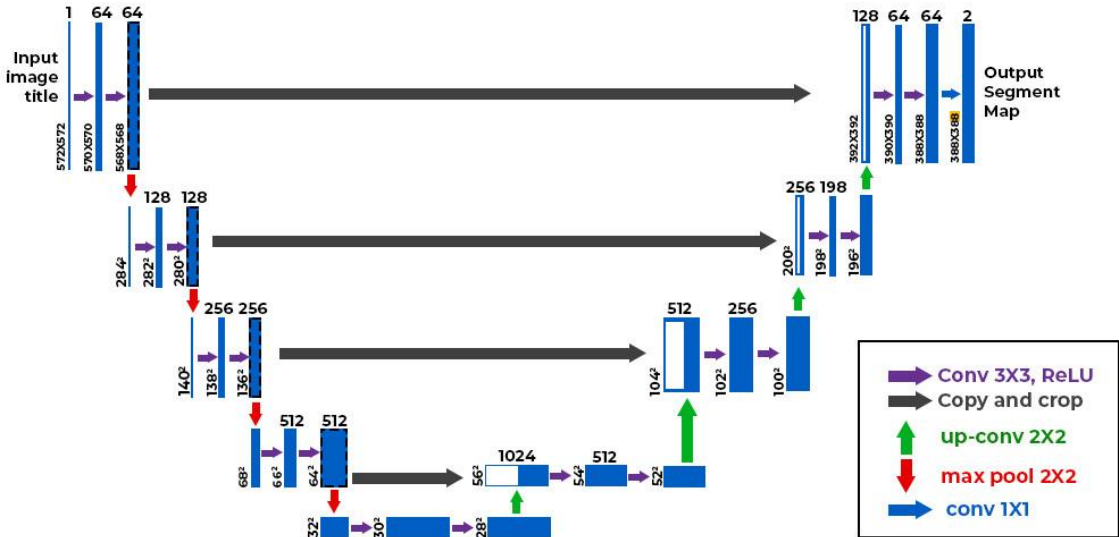


Fig. 3. Neural Network Architecture In Proposed Approaches.

A U-Net network produces a binary segmentation map of size 388×388×2 from a greyscale input image of size 572×572×1. Because no padding is employed, the output is smaller than the input. Padding preserves input size. In the contracting path, the input image's height and breadth drop but its channels increase. The increased channels allow the network to record high-level features along the journey. The bottleneck involves a last convolution step to create a 30x30x1024 feature map. After removing the bottleneck feature map, the expanding path converts it back into the original image size. Upsampling layers increase feature map spatial resolution while lowering channels. The contracting path skip connections assist the decoder layer find and refine image features. Finally, each output pixel labels an object or class in the input image. The output map is a binary segmentation map with foreground and background pixels. Table 4 lists the proposed method levels.

Table 4 - Summarizes The Layer Used In The Proposed Approaches.

Layer Type	Description
Input Layer	Receives the input image as a tensor.
Contracting Path	Down samples the input image to extract high-level features.

In the proposed system, U-Net can perform regression. Although it is for image classification, its convolutional layers can extract features from images to predict continuous variables. To adapt U-Net for regression, some changes are required:

- 1- Replace the last layer: The original U-Net contains a fully connected last layer with 1000 outputs for classification of 1000 categories. Regression requires replacing this layer with a single output neuron to predict continuous variables.
- 2- Customized loss function: Regression tasks use MSE or L1 loss functions instead of cross entropy for classification. The average difference between expected and actual values is measured.
- 3- Fine-tune the network: Regression tasks with transfer learning can start with a pre-trained U-Net. This requires fine-tuning the pre-trained weights of the convolutional layers and freezing the previous layers. This exploits the feature extraction capabilities of the network to adapt it to the regression task.

U-Net was chosen for its exceptional efficacy in medical picture segmentation, its versatility in classification and regression tasks, and its capacity to manage tiny datasets. U-Net is an effective model for pneumonia detection and severity assessment in X-ray images. The layered architecture offers flexibility in layer management, while its sequencing mechanism facilitates extensive training. This is quite beneficial. It was chosen following an extensive review of research publications on deep learning models and the execution of early tests.

7. Evolution Result

In proposed system using confusion matrixes for evolution the result where confusion matrix is a tabular representation that provides a concise summary of how well a machine learning model performs on a given set of test data. It is a method of visually representing the number of correct and incorrect predictions made by the model. It is commonly employed to evaluate the effectiveness of classification models, which seek to forecast a categorical label for each input instance. The matrix presents the count of occurrences generated by the model on the test data. The following point description the Partitioning the four-confusion matrix

- ❖ True Positives (TP) are cases where the model correctly predicts a positive data point.
- True Negatives (TN) are cases where the model correctly predicts a negative data point.
- ❖ False Positives (FP) are cases where the model incorrectly predicts a positive data point.
- ❖ False Negatives (FN) are cases where the model incorrectly predicts a negative data point.

where the use of the confusion matrix, there are key measurements for measuring the efficiency of systems, and these measures vary depending on the four divisions, which is as follows(Mansoor & Al Tamimi, 2022).

Precision: It is the percentage of a group's data that the classifier identifies as belonging to a positive class that is considered accurate, as shown in the precision equation 2 (Heydarian et al., 2022).

$$\text{Precision} = \frac{TP}{TP + FP} \dots\dots\dots (2)$$

- 1- Recall: measurement that determines how accurately a classification system can anticipate the number of affirmative cases. Based on equation 3 (Uddin et al., 2022).

$$\text{Recall (r)} = \frac{TP}{TP + FN} \dots\dots\dots (3)$$

- 2- F1-Score: Precision and retention, as well as the flow of the equation, is denoted by equation 4 (Humphrey et al., 2022).

$$F1 = \frac{2rp}{r + p} = \frac{2 \times TP}{2 \times TP + FP + FN} \dots\dots (4)$$

- 3- Accuracy: measures how close results are to the true or known value. Is denoted by equation 5 (Sayenju & Boardman, 2022)(Najm Mansoor & Al-Tamimi, 2022)

$$\text{Accuracy} = \frac{TP + TN}{TP + FP + TN + FN} \dots\dots\dots (5)$$

- 4- R² (coefficient of determination): measures the percentage of variance in the target variable explained by independent variables in the model. Zero implies no linear relationship between the independent and dependent variables, while 1 indicates a perfect match. A higher R² value suggests the model explains more data variability Is denoted by equation 6 (Gneiting & Resin, 2021)(Achmad Rifa, 2023) (Liu et al., 2022).

$$R^2 = 1 - \Sigma(y_i - \hat{y}_i)^2 / \Sigma(y_i - \bar{y})^2 \dots\dots (6)$$

Where:

y_i is the actual value of the target variable.

\hat{y}_i is the predicted value of the target variable.

\bar{y} is the mean of the actual values.

- 5- RMSE: measures the average model error magnitude. It is the square root of the average squared difference between expected and actual values. Low RMSE means the model produces less errors on average Is denoted by equation 7 (Ashraf et al., 2022) (Li et al., 2022) (Guo et al., 2022).

$$\text{RMSE} = \sqrt{\Sigma(y_i - \hat{y}_i)^2} / n \dots\dots (7)$$

Where:

y_i is the actual value of the target variable

\hat{y}_i is the predicted value of the target variable

n is the number of observations

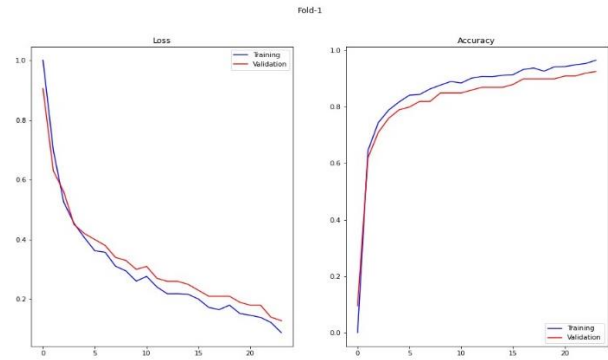
The following section description the result of 5-fold in proposed system as shown in Table 5 and Figure 4.

Table 5 - Result of The Fold

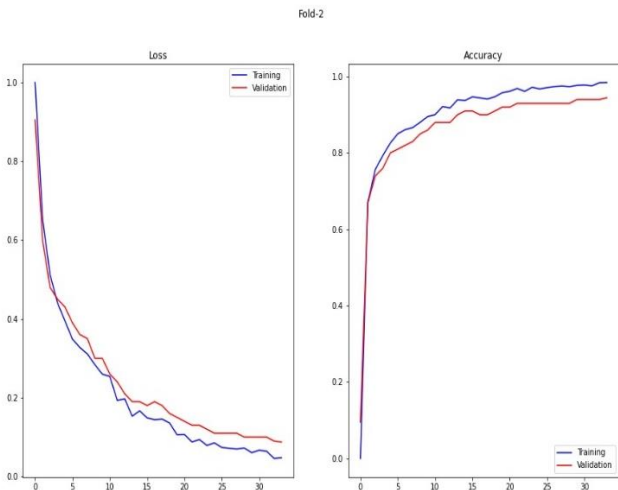
Fold	TP	FN	TN	FP	Accuracy (%)	Precision	Recall	F1-Score
1	209	8	231	22	0.936	0.904	0.963	0.933
2	221	9	230	10	0.959	0.956	0.960	0.958
3	230	4	235	1	0.991	0.995	0.982	0.991
4	229	8	231	2	0.978	0.991	0.966	0.978
5	229	10	229	2	0.974	0.991	0.958	0.974

Result of Diagnosing model

(A)



(B)



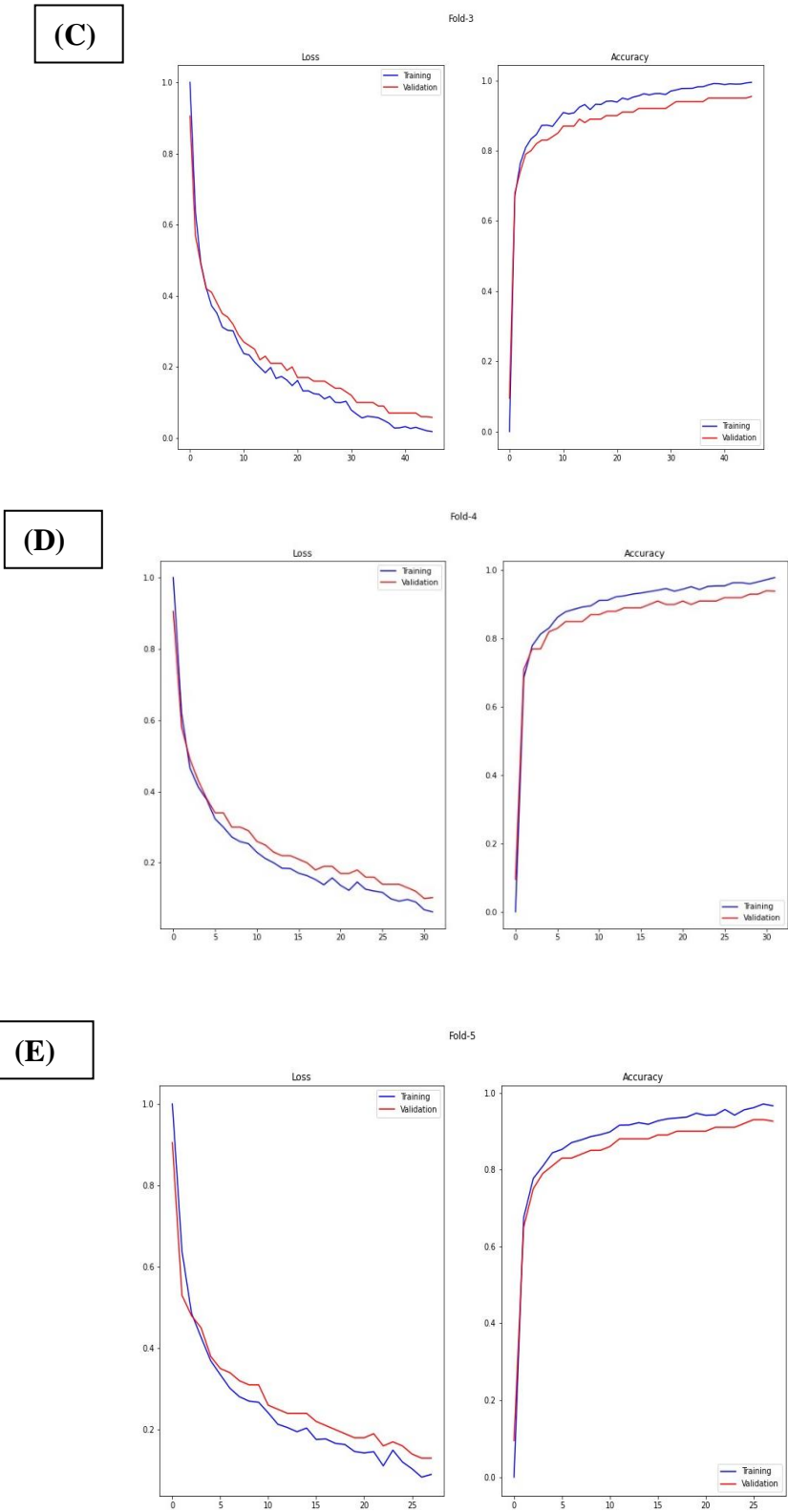


Fig. 4. The Result Of (A) Fold 1, (B)Fold 2, (C)Fold 3, (D)Fold 4, And(E) Fold 5.
based on above result that obtain from proposed system the best fold is 3, Table 6
summarized the result of five-fold in proposed system.

Table 6 - Summarized Of 5-Fold Results	
Fold-1	93.62%
Fold-2	95.96%

Fold-3	99.14%
Fold-4	97.87%
Fold-5	97.45%
The best model is fold 3: 99.14%	

Based on Table above, the results of the five experiments shown were based on the use of k-fold, in which data was divided by 5-fold, in accordance with the size of the dataset, taking 10% as validation of testing. In the end, experiment. (fold-3) was the highest among the results as It was explained in summary form in Figure 5 (a,b,c), as this figure summarized the results obtained regarding the Diagnosing model.

Result of Severity Model (Regression)

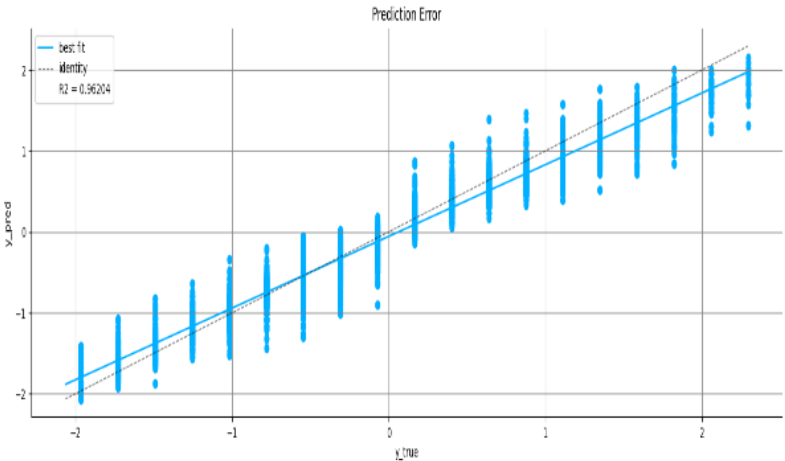


Fig. (5.a). A Chart Shows R2, RMSE And Is Converted into A Table to Extract The Results. The Table Is in CSV Format

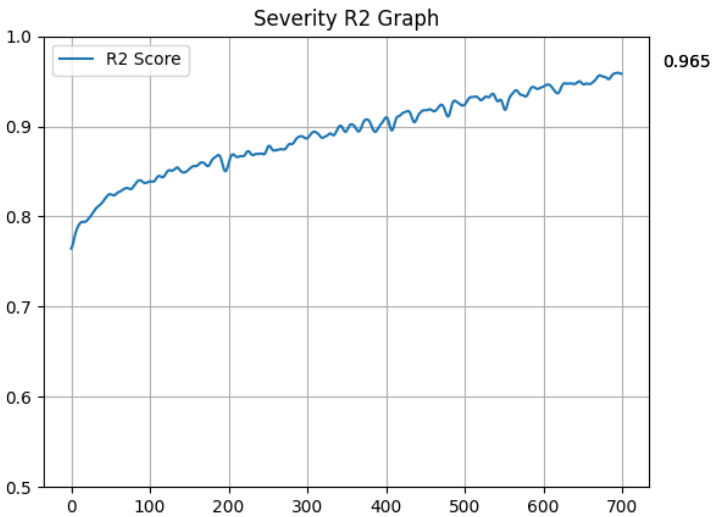


Fig. (5. b). R2 Result of Severity Model in the Training Stage.

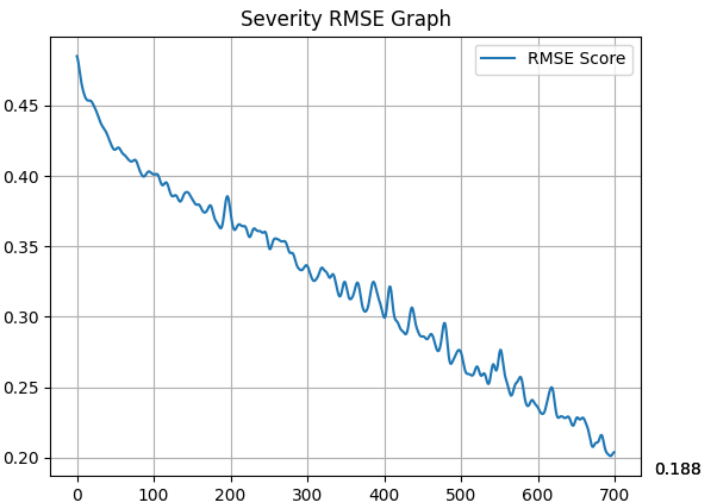


Fig. (5.c). The RMSE result of the risk model in the training stage.

This measure is followed by researchers in building a regression model, which by its nature differs from the measures of the regular model of deep learning or machine learning. Based on the above figures, Table 7 summarizes the results.

Table 7 - Summarizes The Training Stage's Detection Model (Severity) Result

Scale	Result
R2	0.965
REMS	0.188

8. Evolution With Closest Studies

There are many studies related to the topic of diagnosing Corona disease in different ways, but the following is a table 8 showing the two closest approaches to the proposed approach, explaining and summarizing their idea and a comparison with the proposed approach.

Table 8 - Evolution with Closest Studies Using Alexnet Model

Rf.	Idea	Method	Dataset	Result
(Achmad Rifa, 2023)	The research focuses on developing AI tools that can help radiologists or other medical professionals to quickly and accurately diagnose COVID-19 cases. However, the development of such AI tools is difficult due to the lack of publicly available CT and X-ray image datasets. To achieve this goal, the research aims to create a comprehensive dataset of CT scans and X-ray images from various sources and provide a simple but effective COVID-19 detection method using deep learning and transfer learning methods. In this sense, the created X-ray and CT scan image datasets require the application of a modified pre-trained AlexNet model and a basic convolutional neural network (CNN).	AlexNet model CNN	build a comprehensive dataset of X-rays and CT scan images from multiple sources	The result of the experiments shows that the utilized models can provide accuracy up to 98 % via pre-trained network and 94.1 % accuracy by using the modified CNN
(Liu et al.,	The COVID-19 disease was	AlexNet model	An open	Class

2022)	identified and diagnosed using chest X-ray images and a deep learning approach based on a convolutional neural network (CNN). In addition, various scenarios with different types of pooling layers and/or the number of neurons used in the second fully connected layer were proposed for the modified AlexNet design. The chest X-ray images used were collected using two COVID-19 X-ray image datasets, one of which contained a large number of normal and pneumonia X-ray images. Due to the fewer neurons in the second fully connected layer of the proposed model, results equal to or better than the original AlexNet were obtained..	CNN	database of Covid-19 COVID-19 cases with chest X-ray or CT images	Sensitivity= 98.14 Specificity= 99.04 Normal Sensitivity= 72.22 Specificity= 87.60 Abnormal Sensitivity= 90.74 Specificity= 94.89
Proposed system	discuss the diagnosis of infection with Corona disease, whether a person is infected or not, and also determine the infection rate (Severity), that is, the percentage of the virus present in the lungs, based on a global data set of X-rays (X-rays) dedicated to infection, its rate, and its diagnosis by specialized doctors from Through a pre-trained model (U-net model)	U-net model	Covid-19 Xray Severity Scoring	Diagnosis model Accuracy=0.974 Precision=0.991 Recall=0.958 F1-Score=0.974 Severity model R2=0.965 REMS=0.188

The table above highlights the distinction between the proposed methodology and the comparative studies, specifically regarding incidence rate. While all studies concentrated on disease diagnosis, none addressed the determination of infection rates, which is crucial for assessing an individual's infection status and the progression of the disease. The references (Achmad Rifa, 2023) focused on x-rays, CT scans, and two forms of deep learning—neural networks and trained models—yet the research aimed solely to determine an individual's infection status. Additionally, reference(Liu et al., 2022)employed an alternative approach utilizing the Class technique, wherein the system was trained across three classes, aligning with machine learning principles. Exceeding deep learning, as it would be unjust for training and failed to address the injury rate severity. The suggested U-Net with Regression model demonstrates significant enhancements over current methods, especially regarding illness severity evaluation, segmentation, and computing efficiency. The model attains superior accuracy, precision, and recall relative to other leading models. Furthermore, including illness severity analysis into the detection process augments the model's clinical relevance, differentiating it from prior research that concentrated exclusively on detection. The U-Net architecture's capability to delineate infection zones, along with its emphasis on real-time diagnosis, renders it an effective and pragmatic option for pneumonia detection, particularly in resource-constrained environments.

9. Conclusion

Deep learning has enhanced pneumonia detection; nonetheless, challenges such as generalizability across populations, data imbalance, interpretability, quick diagnosis, severity assessment, robustness to noisy data, ethical issues, and model fairness persist. These issues

must be addressed for deep learning to be extensively implemented in clinical practice and to provide precise, equitable, and reliable diagnoses. The efficiency or adoption of the proposed method decides the focus of this investigation. Diseases progress throughout this extensive scientific domain. The prospective advantages of use X-rays for the diagnosis of COVID-19 infection are considerable. This method can enhance early diagnosis, mitigate viral transmission, and improve patient outcomes. With ongoing research and technological advancements, X-ray-based diagnosis of COVID-19 may significantly contribute to addressing this global pandemic. The objective of the scientific study was to elucidate the significance of utilizing artificial intelligence for both viral detection and infection rate assessment, which is crucial for evaluating the severity of the problem. The proposed model yielded encouraging results, and the integration of the image processing technique with a pre-trained model produces equivalent outcomes. A beneficial and effective outcome from selecting the CLAHE filter. In future endeavors, implement the model on an alternative dataset that has not been utilized for training.

References

- Aiadi, O., Khaldi, B., & Saadeddine, C. (2023). MDFNet: an unsupervised lightweight network for ear print recognition. *Journal of Ambient Intelligence and Humanized Computing*, 14(10), 13773-13786.
- Al-Khafaji, R. S., & Al-Tamimi, M. S. (2022). Vein biometric recognition methods and systems: A review. *Advances in Science and Technology. Research Journal*, 16(1), 36-46.
- Al-Tamimi, M. S., & AL-Khafaji, R. S. (2022). Finger vein recognition based on PCA and fusion convolutional neural network. *International Journal of Nonlinear Analysis and Applications*, 13(1), 3667-3681.
- Al-Tamimi, M. S. H., & Sulong, G. (2014). TUMOR BRAIN DETECTION THROUGH MR IMAGES: A REVIEW OF LITERATURE. *Journal of Theoretical & Applied Information Technology*, 62(2).
- Al Jibory, F. K., Mohammed, O. A., & Al Tamimi, M. S. H. (2022). Age estimation utilizing deep learning Convolutional Neural Network. *International Journal on Technical and Physical Problems of Engineering*, 14(4), 219-24.
- AL-Jibory, F. K., Younis, M. A., & Al-Tamimi, M. S. (2022). Preparing of ECG Dataset for Biometric ID Identification with Creative Techniques. *TEM Journal*, 11(4), 1500.
- Alia, A. S., Al-Tamimib, M. S. H., & Ahmed, A. (2020). Secure image steganography through multilevel security. *Image*, 11(1).
- Ariza Cervera, I., Barbancho-Pérez, A. M., Tardón-García, L. J., & Barbancho-Pérez, I. (2023). Energy-based features and bi-LSTM neural network for EEG-based music and voice classification.
- Ashraf, A. H., Imran, M., Qahtani, A. M., Alsufyani, A., Almutiry, O., Mahmood, A., ... & Habib, M. (2022). Weapons detection for security and video surveillance using cnn and YOLO-v5s. *CMC-Comput. Mater. Contin*, 70(4), 2761-2775.
- Chakraborty, S. (2022). APPLICATION OF DEEP LEARNING FOR MEDICAL SCIENCES AND EPIDEMIOLOGY DATA ANALYSIS AND DIAGNOSTIC MODELING.
- Chen, Y., Jiang, G., Li, Y., Tang, Y., Xu, Y., Ding, S., ... & Lu, Y. (2020). A survey on artificial intelligence in chest imaging of COVID-19. *BIO Integration*, 1(3), 137.
- Gayathri, J. L., Abraham, B., Sujarani, M. S., & Ramachandran, S. (2023). A novel CNN framework for the detection of COVID-19 using manta ray optimization and KNN classifier in LUS images. *International Journal of Intelligent Systems and Applications in Engineering*, 11(2), 55-63.
- Gneiting, T., & Resin, J. (2023). Regression diagnostics meets forecast evaluation: Conditional calibration, reliability diagrams, and coefficient of determination. *Electronic Journal of Statistics*, 17(2), 3226-3286.
- Guo, Y., Chen, S., Li, X., Cunha, M., Jayavelu, S., Cammarano, D., & Fu, Y. (2022). Machine learning-based approaches for predicting SPAD values of maize using multi-spectral images. *Remote sensing*, 14(6), 1337.
- Heydarian, M., Doyle, T. E., & Samavi, R. (2022). MLCM: Multi-label confusion matrix. *Ieee*

- Access*, 10, 19083-19095.
- Humphrey, A., Kuberski, W., Bialek, J., Perrakis, N., Cools, W., Nuytens, N., ... & Cunha, P. A. C. (2022). Machine-learning classification of astronomical sources: estimating F1-score in the absence of ground truth. *Monthly Notices of the Royal Astronomical Society: Letters*, 517(1), L116-L120.
- Jiang, X., Gao, T., Zhu, Z., & Zhao, Y. (2021). Real-time face mask detection method based on YOLOv3. *Electronics*, 10(7), 837.
- Jiang, Z., Salcudean, S. E., & Navab, N. (2023). Robotic ultrasound imaging: State-of-the-art and future perspectives. *Medical image analysis*, 89, 102878.
- Kabir, H. D., Abdar, M., Khosravi, A., Jalali, S. M. J., Atiya, A. F., Nahavandi, S., & Srinivasan, D. (2022). Spinalnet: Deep neural network with gradual input. *IEEE Transactions on Artificial Intelligence*, 4(5), 1165-1177.
- Kashyap, G. S., Sohlot, J., Siddiqui, A., Siddiqui, R., Malik, K., Wazir, S., & Brownlee, A. E. (2024). Detection of a facemask in realtime using deep learning methods: Prevention of COVID-19. In *Research Advances in Network Technologies* (pp. 224-240). CRC Press.
- Khalifa, N. E., Loey, M., & Mirjalili, S. (2022). A comprehensive survey of recent trends in deep learning for digital images augmentation. *Artificial Intelligence Review*, 55(3), 2351-2377.
- Kovács, A., Palásti, P., Veréb, D., Bozsik, B., Palkó, A., & Kincses, Z. T. (2021). The sensitivity and specificity of chest CT in the diagnosis of COVID-19. *European radiology*, 31, 2819-2824.
- Lauri, C., Signore, A., Glaudemans, A. W., Treglia, G., Gheysens, O., Slart, R. H., ... & Chakfé, N. (2022). Evidence-based guideline of the European Association of Nuclear Medicine (EANM) on imaging infection in vascular grafts. *European journal of nuclear medicine and molecular imaging*, 49(10), 3430-3451.
- Li, B., Jiang, W., Peng, J., & Li, X. (2022). Deep learning-based remote-photoplethysmography measurement from short-time facial video. *Physiological Measurement*, 43(11), 115003.
- Liu, T., Lough, C. S., Sehhat, H., Ren, Y. M., Christofides, P. D., Kinzel, E. C., & Leu, M. C. (2022). In-situ infrared thermographic inspection for local powder layer thickness measurement in laser powder bed fusion. *Additive Manufacturing*, 55, 102873.
- Mansoor, M., & Al Tamimi, M. (2022). Plagiarism detection system in scientific publication using LSTM networks. *Internacional Journal Technical and physical problems of engineering*, 4(4), 17-24.
- Mehboob, F., Rauf, A., Jiang, R., Saudagar, A. K. J., Malik, K. M., Khan, M. B., ... & AlKhathami, M. (2022). Towards robust diagnosis of COVID-19 using vision self-attention transformer. *Scientific Reports*, 12(1), 8922.
- Mehraeen, E., Alinaghi, S. A. S., Nowroozi, A., Dadras, O., Alilou, S., Shobeiri, P., ... & Karimi, A. (2020). A systematic review of ECG findings in patients with COVID-19. *Indian Heart Journal*, 72(6), 500-507.
- Mijwil, M. M., Aggarwal, K., Doshi, R., Hiran, K. K., & Sundaravadivazhagan, B. (2022). Deep learning techniques for COVID-19 detection based on chest X-ray and CT-scan images: a short review and future perspective. *Asian J Appl Sci*.
- Mansoor, M. N., & Al-Tamimi, M. S. (2022). Computer-based plagiarism detection techniques: A comparative study. *International Journal of Nonlinear Analysis and Applications*, 13(1), 3599-3611.
- Qadir, A. M., Abdalla, P. A., & Abd, D. F. (2024). A Hybrid Lung Cancer Model for Diagnosis and Stage Classification from Computed Tomography Images. *Iraqi Journal for Electrical & Electronic Engineering*, 20(2).
- Rifa'i, A. A. (2023). Impact of Work Discipline on Employee Performance. *Jurnal Ekonomi, Manajemen Dan Akuntansi*, 1(01), 1-8.
- Sayenju, S., Aygun, R., Boardman, J., Don, D. P. R., Zhang, Y., Franks, B., ... & Modgil, G. (2022, January). Directional pairwise class confusion bias and its mitigation. In *2022 IEEE 16th International Conference on Semantic Computing (ICSC)* (pp. 67-74). IEEE.
- Seibert, J. A., & Boone, J. M. (2005). X-ray imaging physics for nuclear medicine technologists. Part 2: X-ray interactions and image formation. *Journal of nuclear*

- medicine technology*, 33(1), 3-18.
- Seibert, J. A., & Boone, J. M. (2005). X-ray imaging physics for nuclear medicine technologists. Part 2: X-ray interactions and image formation. *Journal of nuclear medicine technology*, 33(1), 3-18.
- Shkara, A. A., & Hussain, Y. (2018). Heartbeat Amplification and ECG Drawing from Video (Black and White or Colored Videos). *Iraqi Journal of Science*, 408-419.
- Slika, B., Dornaika, F., Merdji, H., & Hammoudi, K. (2023). Vision transformer-based model for severity quantification of lung pneumonia using chest x-ray images. *arXiv preprint arXiv:2303.11935*.
- Sufian, M. M., Mounq, E. G., Hijazi, M. H. A., Yahya, F., Dargham, J. A., Farzamnia, A., ... & Mohd Naim, N. F. (2023). COVID-19 classification through deep learning models with three-channel grayscale CT images. *Big Data and Cognitive Computing*, 7(1), 36.
- Talukder, M. A., Layek, M. A., Kazi, M., Uddin, M. A., & Aryal, S. (2024). Empowering covid-19 detection: Optimizing performance through fine-tuned efficientnet deep learning architecture. *Computers in Biology and Medicine*, 168, 107789.
- Uddin, S., Haque, I., Lu, H., Moni, M. A., & Gide, E. (2022). Comparative performance analysis of K-nearest neighbour (KNN) algorithm and its different variants for disease prediction. *Scientific Reports*, 12(1), 6256.
- Xu, B., Martín, D., Khishe, M., & Boostani, R. (2022). COVID-19 diagnosis using chest CT scans and deep convolutional neural networks evolved by IP-based sine-cosine algorithm. *Medical & Biological Engineering & Computing*, 60(10), 2931-2949.